HYDROMAGNETIC COUETTE FLOW BETWEEN TWO VERTICAL SEMI-INFINITE PERMEABLE PLATES

COLLINS OWUOR OTIENO

MASTER OF SCIENCE
(Applied Mathematics)

JOMO KENYATTA UNIVERSITY OF AGRICULTURE AND TECHNOLOGY

2021

Hydromagnetic Couette flow between two vertical semi-infinite permeable plates

Collins Owuor Otieno

A Thesis Submitted in Partial Fulfillment of the Requirements for the Degree of Master of Science in Applied Mathematics of the Jomo Kenyatta University of Agriculture and Technology

2021

DECLARATION

This thesis is my original work and has not been submitted for a degree award in any other University.

Signature..... **Date**.....

Collins Owuor Otieno

This thesis has been submitted for examination with our approval as University Supervisors.

Signature..... **Date**.....

Prof. Mathew N. Kinyanjui, PhD

JKUAT, Kenya

Signature..... **Date**.....

Dr. Roy Kiogora, PhD

JKUAT, Kenya

DEDICATION

This Thesis is dedicated to my parents Mr. George Otieno and Mrs. Edwina Otieno, my uncle Dr. Ochieng' Raduma, my siblings Valary Opiyo, Brenda Ogutu and Fiona Awuor.

ACKNOWLEDGMENT

I am highly greatful to my supervisors Prof. M.N. Kinyanjui and Dr. Roy Kiogora of Jomo Kenyatta University of Agriculture and Technology from the Department of Pure and Applied Mathematics for their advice and support in ensuring that this study is a success. Their inspiration, support and knowledge I gathered from them helped me to come up with relevant problem of study. They have ensured that am on the right track in every step.

My appreciation goes to my parents, Mr. George Otieno and Mrs. Edwina Otieno, my uncle Dr. Ochieng' Raduma and family for their encouragement and financial support in my studies.

I also acknowledge the support of my friends Dr. Edward Richard, Mr. Kenneth Muya, Mr. Jared Ogutu, Vellah Onkoba and my course mates Amos, Paul and Chepkonga for their continued encouragement.

Finally, I thank the Almighty God for the gift of life and good health He has given me throughout this course.

TABLE OF CONTENTS

DECLARATION . . . . . **ii**

DEDICATION . . . . . **iii**

ACKNOWLEDGMENT . . . . . **iv**

TABLE OF CONTENTS . . . . . **v**

LIST OF FIGURES . . . . . **vii**

LIST OF APPENDICES . . . . . **ix**

ABBREVIATIONS . . . . . **x**

NOMENCLATURE . . . . . **xi**

GREEK SYMBOLS . . . . . **xii**

ABSTRACT . . . . . **xiii**

CHAPTER ONE: **1**

INTRODUCTION **1**

1.1 Background of the study 1

1.1.1 Background knowledge 1

1.1.2 Definition of key terms 1

1.1.2.1 Fluid 1

1.1.2.2 Couette flow 2

1.1.2.3 Steady and Unsteady flow 2

1.1.2.4 Laminar flow 2

1.1.2.5 Lorentz force 2

1.1.2.6 Viscosity 3

1.1.2.7 Porous medium 3

1.1.2.8 Natural convection 3

1.1.2.9 Buoyancy 3

1.1.3 Non-Dimensionalization 4

1.1.3.1 Reynolds number (Re) 4

1.1.3.2 Prandtl Number (Pr) 4
1.1.3.3 The Eckert number (EC) 5
1.1.3.4 Joules heating parameter (R) 5
1.1.3.5 Magnetic parameter (M) 6
1.2 Statement of the Problem 6
1.3 Justification of the study 7
1.4 Objective of the study 7
1.4.1 General objective 7
1.4.2 Specific objectives 8

CHAPTER TWO: **9**

LITERATURE REVIEW **9**

CHAPTER THREE: **13**

METHODOLOGY **13**
3.1 Model Formulstion 13
3.2 Assumptions 13
3.3 Governing Equations 14
3.3.1 Equation of continuity 14
3.3.2 Electromagnetic equations 15
3.3.2.1 Gauss' Law for Magnetism 15
3.3.2.2 Faraday's law of induction 16
3.3.2.3 Ampere's Law 16
3.3.3 Equation of Momentum 16
3.3.4 Energy Equation 20
3.4 Non-Dimensionalization 22
3.4.1 Initial and boundary conditions 22
3.4.2 Governing equations 23
3.5 Method of Solution 25
3.5.1 Outline of method of solution 25
3.5.2 Advantages of using finite difference method 30

CHAPTER FOUR: **31**

RESULTS AND DISCUSSIONS **31**
4.1 Introduction 31
4.2 Results and Discussions 31
4.2.1 A graph showing the effects of varying Reynolds number on primary velocity 31
4.2.2 A graph showing the effects of varying Magnetic number on primary velocity 31
4.2.3 A graph showing the effects of varying permeability parameter on primary velocity 32
4.2.4 A graph showing the effects of varying Reynolds number on secondary velocity, Re 33
4.2.5 A graph showing the effects of varying permeability parameter on secondary velocity 34
4.2.6 A graph showing the effects of varying Prandtl number on Temperature profile 35
4.2.7 A graph showing the effects of varying Reynolds number on Temperature profile 36
4.2.8 A graph showing the effects of varying Eckert number on Temperature profile 37
4.2.9 A graph showing the effects of varying Joule heating parameter (R) Temperature profile 38
4.3 Validation of Results 39

CHAPTER FIVE: **41**

CONCLUSION AND RECOMENDATIONS **41**
5.1 Introduction 41
5.2 Conclusions 41
5.3 Recommendations 42

REFERENCES **43**

APPENDICES **46**
Published Article 46
MATLAB Codes 47

LIST OF FIGURES

Figure 3.1: Geometry of the flow 13
Figure 3.2: Illustration of the mesh 26

Figure 4.1: Velocity profiles for varied values of the Reynolds number, Re. 32
Figure 4.2: Velocity profiles for varied values of the Magnetic number, M. 33
Figure 4.3: Velocity profiles for varied values of the X number. 34
Figure 4.4: Velocity profiles for varied values of the Reynolds number, Re. 35
Figure 4.5: Velocity profiles for varied values of the x number. 36
Figure 4.6: Temperature profiles for varied values of the Pr number. 37
Figure 4.7: Temperature profiles for varied values of the Re number. 38
Figure 4.8: Temperature profiles for varied values of the Ec number. 39
Figure 4.9: Temperature profiles for varied values of the R number. 40

LIST OF APPENDICES

Appendix I: Published Article 46
Appendix II: MATLAB Codes 47

LIST OF ABBREVIATIONS

MHD	Magnetohydrodynamics
PDE	Partial Differential Equations
FDM	Finite Difference Method
FEM	Finite Element Method
FVM	Finite Volume Method
MATLAB	Matrix Laboratory

LIST OF NOMENCLATURES

SYMBOLS	MEANING
$\overrightarrow{B}$	Magnetic field strength (Wbm^{-2})
B_o	Magnetic flux density (Wbm^{-2})
g	Acceleration due to gravity (ms^{-2})
$\overrightarrow{H}$	Magnetic field intensity (Am^{-1})
$\overrightarrow{J}$	Current density (AM^{-2})
Re	Reynolds number
p	Pressure force (Nm^{-2})
$x^*, y^*, t^*,$	Dimensionless cartesian coordinates
$\overrightarrow{F_i}$	Body forces tensor (N)
$\overrightarrow{V_i}$	Velocity tensor (ms^{-1})
X_j	Space tensor
$\overrightarrow{F_r}$	Electromagnetic force (N)
Pr	Prandtl number
Ha	Hartman number
Q_o	Heat generation constant (Wm^3)
C_p	Specific heat at a constant pressure ($JKg^{-1}k^{-1}$)
T	Temperature (K)
r, θ, z	Cylindrical coordinates

LIST OF GREEK SYMBOLS

SYMBOLS	MEANING
μ	Viscosity$(Kgm^{-1}s^{-1})$
ρ	Fluid density (Kgm^{-3})
η	Dynamic viscosity $(Kgm^{-1}s^{-1})$
ε	Emissivity of black body
σ_{ij}	Normal stresses (Nm^{-2})
τ_{ij}	Shear stresses (Nm^{-2})
σ	Electrical conductivity $(\Omega^{-1}m^{-1})$
μ_e	Magnetic permeability (Hm^{-1})
∇	Gradient Operator

ABSTRACT

In the present study, a hydromagnetic Couette flow between two vertical semi-infinite permeable plates with uniform injection/suction while considering Joule heating has been investigated. The plate where injection takes place is stationary while the other plate moves with a time dependant velocity in the x-direction. Also, a constant magnetic field is applied perpendicular to the stationary plate. The study involves an electrically conducting fluid flow that is incompressibe, viscous and unsteady. The equations that govern the flow which are continuity equation, momentum equation and energy equation were formed and then non-dimensionalised. Due to the non-linear nature of the equations, they cannot be solved analytically and therefore, the method of solution was the finite difference numerical technique because it is more stable and accurate. The results were analyzed and presented graphically. It was established that various non-dimensional parameters such as Joule Heating parameter, Prandtl Number, Eckert Number and other non-dimensional parameters had effects on temperature and velocity profiles which were discussed into details. The effects of varying these parameters led to either increase, decrease or no effect on flow variables. The findings of this study shall be applied in areas such as the design of cooling systems with liquid metal, electrostatic precipitation, purification of crude oil, petroleum industry, aerodynamic heating, polymer technology, accelerators and many others.

CHAPTER ONE

INTRODUCTION

1.1 Background of the study

1.1.1 Background knowledge

MHD Couette flow of an electrically conducting fluid is one of the problems which has received considerable attention due to its varied and wide applications in areas of Geophysics, Astrophysics and fluid engineering fields. The word magneto-hydrodynamic (MHD) is derived from; Magneto which refers to magnetic field while hydro refers liquid and dynamics refers to the motion of a body under influence of forces. Therefore, hydrodynamics refers to the study of fluid that is in motion and the forces that affects the motion while MHD is the study of the dynamics of an electrically conducting fluid in the presence of magnetic field.

Some application areas of interest for this study are in designing of cooling systems with liquid metals, electrostatic precipitation, purification of crude oil, polymer technology among others. The key terms used in the study are defined and discussed into details in the subsection that follows.

1.1.2 Definition of key terms

1.1.2.1 Fluid

A fluid refers to any substance that undergoes continuous deformation when acted upon by an external force. Fluids are classified as liquids or gases. Anderson (2007) from his definition of fluid explained that molecules in a fluid are held together by intermolecular forces such that the fluid tends to possess a volume but no definite shape.

1.1.2.2 Couette flow

Couette flow is a laminar flow of a viscous fluid in the space between two plates which are parallel to each other. One of the plate moves tangetially and the flow is driven by virtue of the viscous drag force which acts on the fluid but may be additionally be motivated by an applied pressure gradient in the flow direction. This type of flow is named in honor of Maurice Marie Alfred Couette, a Professor of Physics in French university of Angers in the late 19^{th} century.

1.1.2.3 Steady and Unsteady flow

Fluid flow can be classified as either steady or unsteady. Steady flow is a flow in which at a particular fixed point, the fluid flow variables such as pressure and temperature do not change with respect to time while unsteady flow is one in which the flow variables at a particular fixed point change with respect to time.
In this study we shall consider unsteady flow scenario.

1.1.2.4 Laminar flow

Laminar flow refers to a flow where there is steady motion of particles of fluid. The fluid flows in parallel layers with no disruption between them. Velocity and viscosity affects the flow in such a way that laminar flow occurs at lower velocities, below the threshold at which the flow becomes turbulent. Turbulent flow is a less orderly flow which results in lateral mixing of fluid layers. The flow of study is laminar flow

1.1.2.5 Lorentz force

The transverse application of a magnetic field to a flow field induces a current and the interaction of this current with the magnetic field generates Lorentz force and according to De Andrade and Pereira (2015), this force opposes the flow and reduces the fluids velocity.

1.1.2.6 Viscosity

According to Ahmed (2015), viscosity of a fluid refers to the measure of its resistance to gradual deformation by shear stress or tensile stress. When the fluid flows through a tube, the particles which compose the fluid generally move more quickly near the tube's axis and more slowly near its walls. Therefore, some stress such as pressure difference between the two ends of the tube is needed to overcome the friction between particle layers to keep the fluid moving. Ideal fluid or inviscid fluid is a fluid that has no resistance to shear stress.

1.1.2.7 Porous medium

Porous medium refers to any material with voids or pores. As defined by Steenbrink and Van der Giessen (2016), porosity or void fraction is the measure of voids in a material. A non-porous material is one that is not permeable to fluids. Permeability is the measure of the ability of a porous material to allow fluids to pass through.

1.1.2.8 Natural convection

Free (or natural) convection is the mode of heat transfer in which the flow is as a result of density gradient created by temperature variation. On the other hand, forced convection occurs when the flow is caused by some external means.

1.1.2.9 Buoyancy

This is the upward force that is exerted by a fluid and it opposes the weight of a partially or fully immersed body. It occurs when there is a changes in density of the fluid. A change in temperature results into a change in density that causes free convection in the fluid. An increase in fluid temperature causes thermal expansion hence a decrease in fluid density. From Archimedes principle where upthrust = ρvg, v represents the volume of the fluid displaced, ρ is the fluid density

and g is the acceleration due to gravity.

1.1.3 Non-Dimensionalization

This is the partial or full removal of units from an equation involving physical quantities using substitution of suitable variables.

Under some similar set of conditions, this process aims at ensuring that the results obtained from a study are applicable to other geometrically similar configurations. This method starts with selecting a suitable scale against which all dimensions in a given physical model are scaled with great generality and mathematical simplicity.

The non-dimensional parameters are discussed as follows;

1.1.3.1 Reynolds number (Re)

Reynold's number is the ratio of inertial forces to viscous forces. It shows the effect on the flowing fluid when the forces changes. At small Reynolds number, there is large viscous forces hence a low velocity flowing fluid. When viscous forces are more dorminant than inertial forces reduces. An increase in Reynold's number shows an increases in the flowing fluid velocity due to a reduction of viscous force of the fluid and this may cause the flow to be turbulent.

Reynolds number is given by:

$$\frac{\rho U_{\infty} H}{\mu} = Re \tag{1.1.1}$$

1.1.3.2 Prandtl Number (Pr)

This is the ratio of the viscous diffusion rate to thermal diffusion.As the Prandtl number tends to one, the velocity boundary layer thickness and the thermal boundary layers are almost of the same thickness. When the Prandtl number is less than 1, the thermal boundary layer is larger than the

velocity boundary layer. For most gaseous substances, the Prandtl number is less than one at standard temperature and pressure. When the Prandtl number of a fluid is more than one, then the velocity boundary layer becomes larger than the thermal boundary layer. Prandtl number is expressed as;

$$Pr = \frac{\rho c_p}{k} \tag{1.1.2}$$

1.1.3.3 The Eckert number (EC)

This is the ratio of the fluid's kinetic energy to thermal internal energy. It shows the rate at which the kinetic energy is converted to internal heat energy due to the resistance of the flowing particles by the viscous forces of the fluid . It is conventionally agreed that when Eckert number is positive, the fluid have gained heat from the surrounding plate hence a rise in temperature of the fluid and vice versa implies a loss of heat from the fluid.

Eckert number is expressed as;

$$Ec = \frac{U_\infty^2}{\rho c_p (T_w - T_\infty)} \tag{1.1.3}$$

1.1.3.4 Joules heating parameter (R)

This is the heating that occurs when an electric current flows in a conductor which has high resistance. The flow of electric current in an electrically resistive conductor causes an increase in temperature in the conductor due to the opposition to the flow of current resulting to more work done to overcome this forces.

This phenomenon is called joule heating which was named after the scientist Prescott Joule, the first scientist to establish Joule law which is expressed as;

$$R = \frac{B_o^2 \sigma \mu}{\rho \mu \rho c_p (T_w - T_\infty)} \tag{1.1.4}$$

1.1.3.5 Magnetic parameter (M)

This is the ratio of magnetic forces acting on a fluid to the viscous forces experienced by the same fluid. The ratio gives the relative significance of resisting forces caused by the magnetic induction and how they affect temperature or velocity profiles of a fluid flow. Magnetic parameter is given as shown below;

$$M = \frac{H \sigma {B_o}^2}{\rho} \tag{1.1.5}$$

1.2 Statement of the Problem

Fluid flows are usually unsteady and take place in presence of both surface forces and body forces. A surface force is a force that acts only on the part of the body which are in contact e.g., pressure gradient, viscous force while a body force is a force which acts on the fluid particles from a distance without physical contact e.g., gravity, electromagnetic force. These forces may either enhance or suppress the fluid motion.

The reality is that the previous research done in this field have a steady/unsteady flow scenario with (or without) the body forces acting on the flow field and have neglected the inclusion of a constant magnetic field applied normal to a stationary plate where injection takes place while considering Joule heating. The analysis of unsteady flows and/or neglecting the body force(s), a constant magnetic field and joule heating in any flow scenario means that some vital pieces of information of engineering interest are neglected.

Therefore this study intends to bridge the gap between the reality and the ideal by addressing the

unsteady hydromagnetic Couette flow between two vertical semi-infinite permeable plates at a constant magnetic field while considering Joule heating.

Thus the present work is an extension of the work of Job and Gunakala (2016).

1.3 Justification of the study

The research on MHD flows is important to science and engineering fields particularly, the influence of a magnetic field on an electrically conducting fluid flow that is incompressible, unsteady and viscous because they are useful in MHD generators, MHD flow meters, heat exchanger, cooling of nuclear reactors, extraction of iron metal from the ores, extrusion plastics in the manufacture of rayon and nylon, etc.

There is need to carry out an analysis on hydromagnetic Couette flow between two vertical semi-infinite plates where a constant magnetic field is applied normally to the main flow while considering Joule heating since the findings shall be beneficial to engineeers in areas such as cooling systems where the walls of a channel containing heated fluid are protected from overheating by passing a cooler fluid through the surface of the channel, in removal of pollutants from plant discharge streams by absorption, electrostatic precipitation and many other useful scientific fields.

1.4 Objective of the study

1.4.1 General objective

To study hydromagnetic Couette flow between two vertical semi-infinite permeable plates.

1.4.2 Specific objectives

1. To model a hydromagnetic Couette flow between two vertical semi-infinite permeable plates with uniform injection and suction where a constant magnetic field is applied perpendicuar to the main flow.

2. To determine the flow variables such as velocity and temperature in profile form.

3. To find the effects of varying the flow parameters such as Joule heating parameter, Prandtl number, Eckert number on the flow variables such as temperature and velocity.

CHAPTER TWO

LITERATURE REVIEW

MHD Couette flow is studied by a number of researchers due to its varied and wide applications in the areas of fluid engineering and astrophysics. The hydromagnetic flow between porous plates has many application areas such as flow meters, in underground energy transport among other areas. Reseachers have studied steady or unsteady flow of an incompressible fluid flow with or without magnetic field and analyzing different aspects of the problem.

Onyango *et al.* (2017) analyzed unsteady hydromagnetic Couette flow with magnetic field lines fixed relative to the moving upper plate and they concluded that magnetic field accelerated the fluid flow when the pressure gradient is constant. It was also found that viscosity exerted a retarding influence on the fluid velocity.

Boniface *et al*. (2014) investigated hydomagnetic steady flow between two infinite parallel vertical porous plates in the presence of a strong magnetic field applied transverse to the direction of the flow. It was concluded that that increase in Prandtl number and the suction parameter led to decrease in fluid temperature. For Grashoff number and magnetic field parameter, their increase caused an increase in velocity while an increase in the suction velocity led to decreased in the velocity of the flow. For the magnetic field parameter, its increase led to the increase in the amplitude of the magnetic field lines.

Seth *et al*. (2017) discussed effect of induced magnetic field on a flow within a porous channel when the fluid flow within the channel is induced due to uniformly accelerated motion when one of the plates starts moving with a time dependent velocity. It was found that magnetic field tends to decrease the velocitty of the fluid in the plate region whereas it reverses the effect on the velocity of the fluid in the region away from the plate. Induced magnetic field tends to be enhanced by chemical reaction in the plate region.

Bodosa and Borkakati (2017) investigated magneto-hydrodynamic Couette flow of an incompressible, viscous and electrically conducting fluid with a uniform transverse magnetic field

acting on the flowing fluid where the fluid flow within the channel is induced due to time dependent movement of one of the plate. They concluded that velocity distribution increases near the plates and then decreases very slowly at the central portion between the plates. They also found out that increase in Prandtl number and Reynolds number led to increase in temperature distributions.

Onyango *et al.* (2015) studied the effects of direction of a transverse magnetic field on unsteady MHD Couette flow with suction and injection. It was concluded that that the direction of the transverse maagnetic field is important as it leads to increased or decreased velocity of the fluid. The injection of the fluid led to increased velocity profile while suction led to decreased velocity of the fluid.

Kinyanjui *et al*. (2013) analyzed MHD Stokes problem for a vertical infinite plate in dissipative rotating fluid with Hall current. The results were that increase in Eckert number, magnetic parameter, rotational parameter led to increase in temperature profile for both free convection cooling of the plate and free convection heating of the plate. Rajput and Sahu (2016) investigated unsteady hydromagnetic Couette flow through a vertical channel in the presence of thermal radiation. They concluded the decrease in velocity profie was brought by an increase in Prandtl number or magnetic number.

Johana *et al*. (2018) investigated unsteady free convection incompressible fluid past a semi-infinite vertical porous plate in the presence of a strong magnetic inclined at an angle α to the plate with Hall and ion-slip current effects. They concluded that increase in Prandtl number led to decrease in both primary and secondary velocities of the flow and temperature profiles.

Attia and Ewis (2010) investigated unsteady MHD Couette flow with heat transfer of a viscoelastic fluid exponential decaying pressure gradient. It was found that the viscoelastic parameter had a marked effect on the temperature and velocity distributions . Also Attia (2018) studied unsteady MHD Couette flow of a viscoelastic fluid with heat transfer and found that the dependence of the temperature on the magnetic field vary with time for all values of the

viscoelastic parameter and higher values of the magnetic field.

Muhuri (2018) investigated Couette magneto-hydrodynamics flow with time varying suction and taking into account the effects of heat and mass transfer.They found that increase in Prandtl number caused a reduction in fluid temperature which resulted into decrease in fluids velocity. Mukhopadhyay (2016) investigated the problem where the fluid flow is confined to porous boundaries with injection and suction. He found that the fluid flow velocity was reduced by suction and on the other hand it was increased by injection. Injection and magnetic field led to reduction of the shear stress at the lower plate.

Chauhan and Agrawal (2015) studied the problem of steady hydromagnetic Couette flow of a highly viscous fluid through a porous channel in the presence of an applied uniform transverse magnetic field and thermal radiation. It was concluded that decrease in temperatue profile was due to increased thermal radiation while increase in velocity profiles was due to increase in magnetic field.

Kim (2018) investigated unsteady MHD convective flow of an incompressible electrially conducting fluid past an infinite vertical porous plate. The numerical results of the study led to conclusion that increase in velocity profiles was due to increased Grashoff number while decrease in velocity profiles was due to increase in Hartman number.

Makinde and Mhone (2019) studied the heat transfer in porous medium in the presence of transverse magnetic field. They analyzed the effects of the heat source parameter and Nusselt number and discovered that the effect of increasing porous parameter leads to increase in Nusselt number.

Jha *et al*. (2015) investigated unsteady natural convective Couette flow of a viscous fluid through a vertical channel. It was that increase in time led to decrease in Nusselt number while on the other had it led to increase in skin friction, temperature and velocity profies. Joseph *et al*. (2015) studied unsteady MHD Couette flow between two infinite parallel plates of an inclined magnetic field with heat transfer. It was found that velocity of the fluid increased due to increased magnetic

number. They also concluded that varying Reynolds number affected the temperature of the fluid flow in that its increase led to increase in the temperature profiles.

Chandran *et al* (2017) did ananysis of unsteady hydromagnetic Couette flow where magnetic field lines were fixed relative to the moving upper plate with suction and injection. It was concluded that the magnetic field, pressure gradient, time and injection have an accelerating influence whereas suction and viscosity exerts a retarding influence on the fluid flow.

Freidoonimehr *et al*. (2015) investigated a turbulent incompressible fluid flow past a semi-infinite vertical plate thati si rotating and an inclined strong magnetic field applied to it. It was concluded that an increase in primary velocity profile was due to increase in the angle of inclination while a decrease in the primary velocity profile was due to increase in the Eckert number.

Raptis and Kafousias (2015) analyzed steady convective MHD fluid flow through parallel semi-infinite plates with constant magnetic field. Hartmann and Prandtl numbers were found to have a great effect in that a decrease in velocity profiles was as a result of increase in Hartman number while the decrease in temperature profiles was due to increase in Prandtl number. Job and Gunakala (2016) studied unsteady magneto-hydrodynamic free convective Couette flow between two vertical permeable plates in the presence of thermal radiation using Galerkin's finite method. They concluded that increase in radiation parameter led to decrease in velocity profiles at small time but increases them at large time. Both the temperature and velocity profiles increased due to increase in Prandtl number, Eckert number and Reynolds number.

This study therefore tends to extend the work of Job and Gunakala (2016) with consideration of a constant magnetic field applied relative to the stationary plate and the other plate where the suction takes place is on motion and incorporating joule heating.

CHAPTER THREE

METHODOLOGY

3.1 Model Formulstion

This study considers an incompressible, electrically conducting, viscous and unsteady fluid flow between two parallel vertical plates along z = 0 and z = h. The plates are of semi-infinite in length in the x-direction.

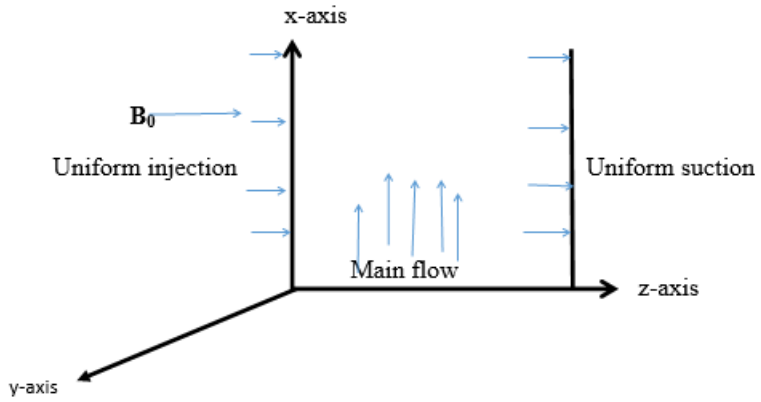

Figure 3.1: Geometry of the flow

Initially, at time $t = 0$, both the plates and fluid are stationary at temperature T_0. When $t > 0$ the plate along z = h starts moving with time-dependent velocity $U_0 t^c$ in the direction of the main flow where U_0 is a constant and c is a non-negative integer and its temperature rises to T_1 while the other plate located at z = 0 remains stationary with its temperature maintained at T_0. A constant magnetic field B_0 is applied normal to the x-axis.

The following assumptions have been used to simplify the problem.

3.2 Assumptions

They are as follows;

1. The fluid is incompressible, that is, the density is assumed to be a constant.

2. The fluid flow is two-dimensional.

3. The fluid flow is laminar.

4. There is no chemical reaction.

5. Coefficient of viscosity, electrical conductivity and thermal conductivity are constant.

6. There is negligible force due to electric field since there is no current applied.

3.3 Governing Equations

The fundamentals of fluid dynamics are based on universal laws that govern fluid flows. The governing equations for this study are continuity equation, momentum equation, equation of energy and the electromagnetic equations.

3.3.1 Equation of continuity

This equation is derived from the law of conservation of mass. It states that, mass can neither be created nor destroyed under normal conditions. It is derived by taking a mass balance on the fluid entering and leaving a volume element in the flow field. The general equation of continuity of a fluid flow is given :

$$\frac{\partial \rho}{\partial t} + \overrightarrow{\nabla}.(\rho \overrightarrow{q}) = 0 \tag{3.3.1}$$

where $\overrightarrow{q} = u\hat{i} + v\hat{j} + w\hat{k}$ is the velocity vector in the x,y and z-directions.

In tensor form the equation is:

$$\frac{\partial \rho}{\partial t} + \frac{\partial}{\partial x_i}(\rho u_i) = 0 \tag{3.3.2}$$

Since density is assumed to be constant, then the equation becomes

$$\rho \frac{\partial u_i}{\partial x_i} = 0 \tag{3.3.3}$$

which in component form is given by

$$\frac{\partial u}{\partial x} + \frac{\partial v}{\partial y} + \frac{\partial w}{\partial z} = 0 \tag{3.3.4}$$

since the flow is in 2-dimensional in z and x direction, the equation becomes

$$\frac{\partial u}{\partial x} + \frac{\partial w}{\partial z} = 0 \tag{3.3.5}$$

3.3.2 Electromagnetic equations

These equations give the relationship between the magnetic field intensity $\overrightarrow{H}$, the induction current density vector $\overrightarrow{J}$, the electric field intensity $\overrightarrow{E}$, the electric displacement $\overrightarrow{D}$ and the magnetic induction vector $\overrightarrow{B}$.

The basic electromagnetic equations are as follows:

3.3.2.1 Gauss' Law for Magnetism

Gauss' law basically states that all magnetic fields, $\overrightarrow{B}$ have field lines that are continuous.

$$\nabla . \overrightarrow{B} = 0 \tag{3.3.6}$$

3.3.2.2 Faraday's law of induction

This law states that changes in magnetic fields induces an electric field. It is basically used to predict how magnetic field interact with electric current to produce electromotive force.

$$\nabla \times \overrightarrow{E} = \frac{\partial \overrightarrow{B}}{\partial t} \tag{3.3.7}$$

where

$$\overrightarrow{B} = \mu_e \overrightarrow{H} \tag{3.3.8}$$

3.3.2.3 Ampere's Law

This Law states that, for any closed loop path, then the product of thr sum of the length elements and the magnetic field in the direction of the length element is equal to the product of permeability and the electric current within an enclosed loop.

$$\nabla \times \overrightarrow{H} = \overrightarrow{J} \tag{3.3.9}$$

$$\nabla . \overrightarrow{D} = \rho_e \tag{3.3.10}$$

3.3.3 Equation of Momentum

The equation is derived from the Newton's second law of motion which requires that the sum of all the force acting on a control volume must be equal to the rate of change time of fluid momentum within that control volume.

$$\frac{\partial \overrightarrow{q}}{\partial t} + \overrightarrow{q}\left(\overrightarrow{\nabla} . \overrightarrow{q}\right) = -\frac{1}{\rho}\overrightarrow{\nabla} p + \frac{\mu}{\rho}\nabla^2 \overrightarrow{q} + \overrightarrow{F}_i \tag{3.3.11}$$

where $\overrightarrow{\nabla} p$ represents the pressure gradient of the flow, $\mu\nabla^2\overrightarrow{q}$ is the viscous force term, $\overrightarrow{F}_i$ is the body forces acting on the flow, $\overrightarrow{q}\left(\overrightarrow{\nabla}.\overrightarrow{q}\right)$ is the convective acceleration that is due to change in space co-ordinates, $\frac{\partial\overrightarrow{q}}{\partial t}$ is the temporal acceleration due to change in time.

The body forces includes magnetic and gravitational forces will be included as follows:

$$\frac{\partial\overrightarrow{q}}{\partial t}+\overrightarrow{q}\left(\overrightarrow{\nabla}.\overrightarrow{q}\right)=-\frac{1}{\rho}\overrightarrow{\nabla}p+\frac{\mu}{\rho}\nabla^2\overrightarrow{q}+\rho g+\frac{\vec{J}\times\vec{B}}{\rho} \tag{3.3.12}$$

Lorentz force is given by:

$$F=\vec{J}\times\vec{B} \tag{3.3.13}$$

where

$$\vec{J}=\sigma(\vec{E}+q\times\vec{B}) \tag{3.3.14}$$

But $\vec{E}=0$ because there is no externally applied electric field, thus

$$\vec{J}=\sigma(\vec{q}\times\vec{B}) \tag{3.3.15}$$

now

$$\vec{J}=\sigma\begin{vmatrix} i & j & k \\ u & v & w \\ B_x & B_y & B_z \end{vmatrix} \tag{3.3.16}$$

the flow is two dimensional and the magnetic fields have been applied perpendicularly to the main flow.

$$\vec{J}=\sigma\begin{vmatrix} i & j & k \\ u & 0 & w \\ 0 & 0 & B_o \end{vmatrix}=-\sigma uB_o j \tag{3.3.17}$$

$$\vec{F} = \vec{J} \times \vec{B} = \begin{vmatrix} i & j & k \\ 0 & -\sigma u B_o & 0 \\ 0 & 0 & B_o \end{vmatrix} = -\sigma u B_o^2 i \tag{3.3.18}$$

replacing (3.3.18) in the equation(3.3.12) , it becomes

$$\frac{\partial \overrightarrow{q}}{\partial t} + \overrightarrow{q}\left(\overrightarrow{\nabla}.\overrightarrow{q}\right) = -\frac{1}{\rho}\overrightarrow{\nabla} p + \frac{\mu}{\rho}\nabla^2 \overrightarrow{q} + \rho g - \frac{\sigma u B_o^2}{\rho} \tag{3.3.19}$$

When the fluid is heated, the volume of the fluid that is displaced equals to the expanded fluid due to the thermal expansion. This is given by:

$$v = \beta(T - T_\infty) \tag{3.3.20}$$

where β is the coefficient of thermal expansion.

where upthrust=Buoyancy:

$$\rho(\beta(T - T_\infty))g = \beta\rho g(T - T_\infty) \tag{3.3.21}$$

incorporating buoyancy effects in the equation motion given by (3.3.19) becomes

$$\frac{\partial \overrightarrow{q}}{\partial t} + \overrightarrow{q}\left(\overrightarrow{\nabla}.\overrightarrow{q}\right) = -\frac{1}{\rho}\overrightarrow{\nabla} p + \frac{\mu}{\rho}\nabla^2 \overrightarrow{q} + \rho g - \frac{\sigma u B_o^2}{\rho} + \beta g(T - T_\infty) \tag{3.3.22}$$

The sum of the pressure term in the momentum equation and the gravitational force gives the porosity term as given in darcy equation:

$$-\nabla p + \rho g = \frac{\mu}{k_p} q \tag{3.3.23}$$

putting equation (3.3.23) on (3.3.22) it becomes

$$\frac{\partial \overrightarrow{q}}{\partial t} + \overrightarrow{q}\left(\overrightarrow{\nabla}.\overrightarrow{q}\right) = \frac{\mu}{k_p}q + \frac{\mu}{\rho}\nabla^2\overrightarrow{q} - \frac{\sigma u B_o^2}{\rho} + \beta g(T - T_\infty) \tag{3.3.24}$$

since velocity is given in u and w, rewriting (3.3.24) into x and z components the following are obtained

The momentum equation along the x-axis is given by

$$\frac{\partial u}{\partial t} + \vec{q}\left(\overrightarrow{\nabla}.\vec{u}\right) = \frac{\mu}{k_p}u + \frac{\mu}{\rho}\nabla^2 u - \frac{\sigma u B_o^2}{\rho} + \beta g(T - T_\infty) \tag{3.3.25}$$

The momentum equation along the z-axis and using the fact that the magnetic field is parallel to z-axis, then

$$\frac{\partial w}{\partial t} + \vec{q}\left(\overrightarrow{\nabla}.\vec{w}\right) = \frac{\mu}{k_p}w + \mu\nabla^2 w \tag{3.3.26}$$

but

$$\nabla = i\frac{\partial}{\partial x} + k\frac{\partial}{\partial z} \tag{3.3.27}$$

and

$$\nabla^2 = \frac{\partial^2}{\partial x^2} + \frac{\partial^2}{\partial z^2} \tag{3.3.28}$$

Using equations (3.3.27) and (3.3.28) on equation (3.3.25) it becomes

$$\frac{\partial u}{\partial t} + u\frac{\partial u}{\partial x} + w\frac{\partial u}{\partial z} = \frac{\mu}{k_p}u + \frac{\mu}{\rho}\left(\frac{\partial^2 u}{\partial x^2} + \frac{\partial^2 u}{\partial z^2}\right) - \frac{\sigma u B_o^2}{\rho} + \beta g(T - T_\infty) \tag{3.3.29}$$

Using equations (3.3.27) and (3.3.28) on equation (3.3.26) it becomes

$$\frac{\partial w}{\partial t}+u\frac{\partial w}{\partial x}+w\frac{\partial w}{\partial z}=\frac{\mu}{k_p}w+\frac{\mu}{\rho}\left(\frac{\partial^2 w}{\partial x^2}+\frac{\partial^2 w}{\partial z^2}\right) \tag{3.3.30}$$

Incorporating constant suction and injection in equations (3.3.29) and (3.3.30) becomes

$$\frac{\partial u}{\partial t}+u\frac{\partial u}{\partial x}+w_0\frac{\partial u}{\partial z}=\frac{\mu}{k_p}u+\frac{\mu}{\rho}\left(\frac{\partial^2 u}{\partial x^2}+\frac{\partial^2 u}{\partial z^2}\right)-\frac{\sigma u B_o^2}{\rho}+\beta g(T-T_\infty) \tag{3.3.31}$$

$$\frac{\partial w}{\partial t}+u\frac{\partial w}{\partial x}+w_0\frac{\partial w}{\partial z}=\frac{\mu}{k_p}w+\frac{\mu}{\rho}\left(\frac{\partial^2 w}{\partial x^2}+\frac{\partial^2 w}{\partial z^2}\right) \tag{3.3.32}$$

3.3.4 Energy Equation

This equation is drawn from the principle of conservation of energy which states that energy neither be created nor destroyed but can only be transformed from one form to the other. The first law of Thermodynamic states that the amount of heat added to a system equals the change in internal energy plus work done, that is $dE = dQ - dW$.

Since the fluid is incompressible, the energy equation is expressed as;

$$\rho c_p\frac{DT}{Dt}=K\nabla^2 T+\mu\Phi+\frac{J^2}{\sigma} \tag{3.3.33}$$

Where K is a constant fluid conductivitty, c_p is specific heat capacity at constant pressure, $\frac{DT}{Dt}$ is the material derivative, $\mu\Phi$ is the internal heating due to viscous dissipation and $(\frac{J^2}{\sigma})$ is the ohmic heating due to resistance of the electrolyte. $\mu\Phi$ is the viscous dissipation term which is given by:

$$\begin{aligned}\mu\phi = 2\mu((\frac{\partial u}{\partial x})^2+\mu(\frac{\partial v}{\partial y})^2+\mu(\frac{\partial w}{\partial z})^2)+\mu((\frac{\partial u}{\partial y}+\frac{\partial v}{\partial x})^2+\mu(\frac{\partial v}{\partial z}+\frac{\partial w}{\partial y})^2+\\ \mu(\frac{\partial w}{\partial x}+\frac{\partial u}{\partial z})^2)-\frac{2}{3}\mu(\frac{\partial u}{\partial x}+\frac{\partial v}{\partial y}+\frac{\partial w}{\partial z})\end{aligned} \tag{3.3.34}$$

The term above reduces to equation (3.3.35) since from the equation of continuity $\frac{\partial u}{\partial x} + \frac{\partial w}{\partial z} = 0$ and the flow is two dimensional along x and w only.

$$\mu\phi = \mu\left[(\frac{\partial u}{\partial x})^2 + (\frac{\partial w}{\partial z})^2\right] \tag{3.3.35}$$

substituting (3.3.35) on (3.3.36)

$$\rho c_p \frac{DT}{Dt} = K\nabla^2 T + \mu\left[(\frac{\partial u}{\partial x})^2 + (\frac{\partial w}{\partial z})^2\right] + \frac{J^2}{\sigma} \tag{3.3.36}$$

Computing Joule heating

$$J = -\sigma u B_0 i \tag{3.3.37}$$

$$\frac{J^2}{\sigma} = \frac{\sigma^2 u^2 B_0^2}{\sigma} = \sigma u^2 B_0^2 \tag{3.3.38}$$

$$\nabla^2 = \frac{\partial^2}{\partial x^2} + \frac{\partial^2}{\partial z^2} \tag{3.3.39}$$

substituting equation (3.3.38) and equation (3.3.39) on equation of energy (3.3.36) becomes

$$\rho c_p\left[\frac{\partial T}{\partial t} + u\frac{\partial T}{\partial x} + w\frac{\partial T}{\partial z}\right] = K\left[\frac{\partial^2 T}{\partial x^2} + \frac{\partial^2 T}{\partial z^2}\right] + \mu\left[(\frac{\partial u}{\partial x})^2 + (\frac{\partial w}{\partial z})^2\right] + \sigma u^2 B_0^2 \tag{3.3.40}$$

dividing all through by ρc_p

$$\left[\frac{\partial T}{\partial t} + u\frac{\partial T}{\partial x} + w\frac{\partial T}{\partial z}\right] = \frac{K}{\rho c_p}\left[\frac{\partial^2 T}{\partial x^2} + \frac{\partial^2 T}{\partial z^2}\right] + \frac{\mu}{\rho c_p}\left[(\frac{\partial u}{\partial x})^2 + (\frac{\partial w}{\partial z})^2\right] + \frac{\sigma u^2 B_0^2}{\rho c_p} \tag{3.3.41}$$

3.4 Non-Dimensionalization

This is done by first selecting characteristic dimensionless quantities which are the substituted into the governing equations. The following non-dimensional quantities were used to non-dimensionalize the governing equations;

$$u^* = \frac{u}{U_\infty}, \quad w^* = \frac{w}{U_\infty}, \quad w_0^* = \frac{w_0}{U_\infty}, \quad t^* = \frac{U_\infty t}{h}, \quad x^* = \frac{x}{h}, \quad z^* = \frac{z}{h}, \quad T^* = \frac{T - T_\infty}{T_w - T_\infty}$$

$$u = U_\infty u^*, w = U_\infty w^*, w_0 = U_\infty w_0^*, t = \frac{h}{U_\infty} t^*, x = h x^*, z = h z^*, T = (T_w - T_\infty) T^* + T_\infty$$

The following partial derivatives in non-dimensional form will be substituted into equations (3.3.31), (3.3.32) and (3.3.41):

3.4.1 Initial and boundary conditions

At the entrance at $0 \leq z \leq H$

$$t^* \leq 0;\ u^* = 0,\ v^* = 0,\ w^* = 0, T^* = 0 \tag{3.4.1}$$

$$t^* > 0,\ u^* = 1, v^* = 0, T^* = 1 \tag{3.4.2}$$

At the exit:

$$t^* \geq 0,\ u^* = \frac{u}{U_\infty} and\ u = cx^2\ and\ x = Hx^* \tag{3.4.3}$$

$$u^* = \frac{cx^2}{U_\infty}\ thus\ u^* = c\frac{(Hx^*)^2}{U_\infty}, v^* = 0\ and\ w^* = w_0^* \tag{3.4.4}$$

$$T = T_w\ and\ T^* = \frac{T - T_\infty}{T_w - T_\infty} = \frac{T_w - T_\infty}{T_w - T_\infty} = 1 \tag{3.4.5}$$

At the other surface:

$$t > 0, u^* = 0, v^* = 0, T = T_\infty \; and \; T^* = \frac{T_\infty - T_\infty}{T_w - T_\infty} = 0 \tag{3.4.6}$$

3.4.2 Governing equations

$$\frac{\partial u}{\partial t} = \frac{\partial u}{\partial u^*}\frac{\partial u^*}{\partial t^*}\frac{\partial t^*}{\partial t} = \frac{U_\infty^2}{h}\frac{\partial u^*}{\partial t^*} \tag{3.4.7}$$

$$\frac{\partial u}{\partial x} = \frac{\partial u}{\partial u^*}\frac{\partial u^*}{\partial x^*}\frac{\partial x^*}{\partial x} = U_\infty\frac{\partial u^*}{\partial x^*}\frac{1}{h} = \frac{U_\infty}{h}\frac{\partial u^*}{\partial x^*} \tag{3.4.8}$$

$$\frac{\partial u}{\partial z} = \frac{\partial u}{\partial u^*}\frac{\partial u^*}{\partial z^*}\frac{\partial z^*}{\partial z} = U_\infty\frac{\partial u^*}{\partial z^*}\frac{1}{h} = \frac{U_\infty}{h}\frac{\partial u^*}{\partial z^*} \tag{3.4.9}$$

$$\frac{\partial^2 u}{\partial x^2} = \frac{\partial}{\partial x}(\frac{\partial u}{\partial x}) = \frac{\partial}{\partial x}(\frac{U_\infty}{h}\frac{\partial u^*}{\partial x^*}) = \frac{\partial}{\partial x^*}(\frac{U_\infty}{h}\frac{\partial u^*}{\partial x}) = \frac{\partial}{\partial x^*}(\frac{U_\infty}{h}\frac{\partial u^*}{\partial x^*}\frac{\partial x^*}{\partial x}) = \frac{U_\infty}{h^2}\frac{\partial^2 u^*}{\partial x^{*2}} \tag{3.4.10}$$

$$\frac{\partial^2 u}{\partial z^2} = \frac{\partial}{\partial z}(\frac{\partial u}{\partial z}) = \frac{\partial}{\partial z}(\frac{U_\infty}{h}\frac{\partial u^*}{\partial z^*}) = \frac{U_\infty}{h^2}\frac{\partial^2 u^*}{\partial z^{*2}} \tag{3.4.11}$$

$$\frac{\partial w}{\partial t} = \frac{U_\infty^2}{h}\frac{\partial w^*}{\partial t^*} \tag{3.4.12}$$

$$\frac{\partial w}{\partial x} = \frac{U_\infty}{h}\frac{\partial w*}{\partial x^*} \tag{3.4.13}$$

$$\frac{\partial w}{\partial z} = \frac{U_\infty}{h}\frac{\partial w^*}{\partial z^*} \tag{3.4.14}$$

$$\frac{\partial^2 w}{\partial x^2} = \frac{U_\infty}{h^2}\frac{\partial^2 w^*}{\partial x^{*2}} \tag{3.4.15}$$

$$\frac{\partial^2 w}{\partial z^2} = \frac{U_\infty}{h^2}\frac{\partial^2 w^*}{\partial z^{*2}} \tag{3.4.16}$$

$$\frac{\partial T}{\partial t} = \frac{\partial T}{\partial T^*}\frac{\partial T^*}{\partial t^*}\frac{\partial t^*}{\partial t} = (T_w - T_\infty)\frac{\partial T^*}{\partial t^*}\frac{U_\infty}{h} = \frac{U_\infty}{h}(T_w - T_\infty)\frac{\partial T^*}{\partial t^*} \tag{3.4.17}$$

$$\frac{\partial T}{\partial x} = \frac{\partial T}{\partial T^*}\frac{\partial T^*}{\partial x^*}\frac{\partial x^*}{\partial x} = \frac{(T_w - T_\infty)}{h}\frac{\partial T^*}{\partial x^*} \tag{3.4.18}$$

$$\frac{\partial T}{\partial z} = \frac{\partial T}{\partial T^*}\frac{\partial T^*}{\partial z^*}\frac{\partial z^*}{\partial z} = \frac{(T_w - T_\infty)}{h}\frac{\partial T^*}{\partial z^*} \tag{3.4.19}$$

$$\frac{\partial^2 T}{\partial z^2} = \frac{(T_w - T_\infty)}{h^2}\frac{\partial^2 T^*}{\partial z^{*2}} \tag{3.4.20}$$

$$\frac{\partial^2 T}{\partial x^2} = \frac{(T_w - T_\infty)}{h^2}\frac{\partial^2 T^*}{\partial x^{*2}} \tag{3.4.21}$$

Substituting the partial derivatives (3.4.7),(3.4.8),(3.4.9),(3.4.10) and (3.4.11) to the momentum equations (3.3.31) becomes:

$$\frac{\partial u^*}{\partial t^*} + u^*\frac{\partial u^*}{\partial x^*} + w_o^*\frac{\partial u^*}{\partial z^*} = \frac{1}{Re}(\frac{\partial^2 u^*}{\partial x^{*2}} + \frac{\partial^2 u^*}{\partial z^{*2}}) - Mu^* - Xu^* + GrT^* \tag{3.4.22}$$

The equation (3.4.22) represent momentum equation in x-direction.

Substituting the partial derivatives (3.4.12),(3.4.13),(3.4.14),(3.4.15) and (3.4.16) to the momentum equations (3.3.32) becomes:

$$\frac{\partial w^*}{\partial t^*} + u^*\frac{\partial w^*}{\partial x^*} + w_o^*\frac{\partial w^*}{\partial z^*} = \frac{1}{Re}(\frac{\partial^2 w^*}{\partial x^{*2}} + \frac{\partial^2 w*}{\partial z^{*2}}) - Xw^* \tag{3.4.23}$$

The equation (3.4.23) represent momentum equation in z-direction.

Substituting the partial derivatives (3.4.17),(3.4.18),(3.4.19),(3.4.20) and (3.4.21) to the energy

equations (3.3.41) becomes:

$$\frac{\partial T^*}{\partial t^*} + u^* \frac{\partial T^*}{\partial x^*} + w_o^* \frac{\partial T^*}{\partial z^*} = \frac{1}{Re}\frac{1}{Pr}\left(\frac{\partial^2 T^*}{\partial x^{*2}} + \frac{\partial^2 T^*}{\partial z^{*2}}\right) + \frac{Ec}{Re}\left(\left(\frac{\partial u^*}{\partial x^*}\right)^2 + \left(\frac{\partial w^*}{\partial x^*}\right)^2\right)$$

$$+ Re.R(u^*)^2 \tag{3.4.24}$$

The equation (3.4.24) represent the energy equation .

3.5 Method of Solution

3.5.1 Outline of method of solution

The numerical approximation method of finite differences is the proposed method of solving the system of the non-linear equations that are obtained from thuis particular flow problem. A finite difference grid is developed where each modal point identified by a double index (i, j) that define its location with respect to t and x as shown in the figure 3.2.

The grid is to calculate the values at the mesh points.

The finite difference approximations of $\frac{\partial U}{\partial t}$, $\frac{\partial U}{\partial x}$, $\frac{\partial U}{\partial z}$, $\frac{\partial^2 U}{\partial x^2}$, and $\frac{\partial^2 U}{\partial z^2}$ at k and k+1 are given by:

$$\frac{\partial U}{\partial t} = \frac{U_{i,j}^{k+1} - U_{i,j}^{k}}{\Delta t} \tag{3.5.1}$$

$$\frac{\partial U}{\partial x} = \frac{U_{i+1,j}^{k+1} - U_{i-1,j}^{k+1} + U_{i+1,j}^{k} - U_{i-1,j}^{k}}{4(\Delta x)} \tag{3.5.2}$$

$$\frac{\partial U}{\partial z} = \frac{U_{i,j+1}^{k+1} - U_{i,j-1}^{k+1} + U_{i,j+1}^{k} - U_{i,j-1}^{k}}{4(\Delta z)} \tag{3.5.3}$$

$$\frac{\partial^2 U}{\partial x^2} = \frac{U_{i+1,j}^{k+1} - 2U_{i,j}^{k+1} + U_{i-1,j}^{k+1} + U_{i+1,j}^{k} - 2U_{i,j}^{k} + U_{i-1,j}^{k}}{2(\Delta x)^2} \tag{3.5.4}$$

$$\frac{\partial^2 U}{\partial z^2} = \frac{U_{i,j+1}^{k+1} - 2U_{i,j}^{k+1} + U_{i,j-1}^{k+1} + U_{i,j+1}^{k} - 2U_{i,j}^{k} + U_{i,j-1}^{k}}{2(\Delta z)^2} \tag{3.5.5}$$

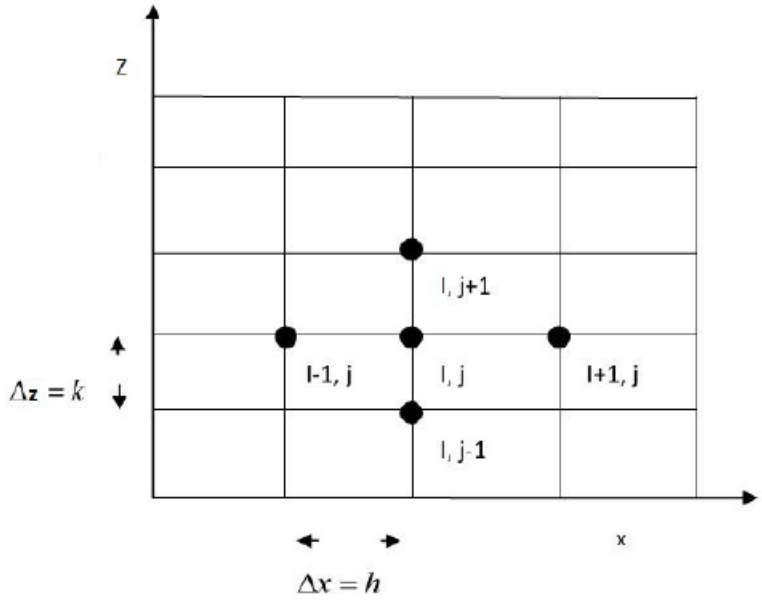

Figure 3.2: Illustration of the mesh

Substituting these in equation of momentum (3.4.22) yields:

$$\frac{U_{i,j}^{k+1}-U_{i,j}^{k}}{\Delta t}+U_{i,j}^{k+1}\left(\frac{U_{i+1,j}^{k+1}-U_{i-1,j}^{k+1}+U_{i+1,j}^{k}-U_{i-1,j}^{k}}{4(\Delta x)}\right)+w_0\left(\frac{U_{i,j+1}^{k+1}-U_{i,j-1}^{k+1}+U_{i,j+1}^{k}-U_{i,j-1}^{k}}{4(\Delta z)}\right)$$
$$=\frac{1}{Re}\left(\frac{U_{i+1,j}^{k+1}-2U_{i,j}^{k+1}+U_{i-1,j}^{k+1}+U_{i+1,j}^{k}-2U_{i,j}^{k}+U_{i-1,j}^{k}}{2(\Delta x)^2}\right)$$
$$+\frac{1}{Re}\left(\frac{U_{i,j+1}^{k+1}-2U_{i,j}^{k+1}+U_{i,j-1}^{k+1}+U_{i,j+1}^{k}-2U_{i,j}^{k}+U_{i,j-1}^{k}}{2(\Delta z)^2}\right)-XU_{i,j}^{k+1}-MU_{i,j}^{k+1}+GrT_{i,j}^{k+1} \tag{3.5.6}$$

Making $U_{i,j}^{k+1}$ yields:

$$U_{i,j}^{k+1} = \left[\frac{U_{i,j}^{k}}{\Delta t} - w_0 \left(\frac{U_{i,j+1}^{k+1} - U_{i,j-1}^{k+1} + U_{i,j+1}^{k} - U_{i,j-1}^{k}}{4(\Delta z)} \right) + GrT_{i,j}^{k+1} + \right.$$
$$\left. \frac{1}{Re} \left(\frac{U_{i+1,j}^{k+1} + U_{i-1,j}^{k+1} + U_{i+1,j}^{k} - 2U_{i,j}^{k} + U_{i-1,j}^{k}}{2(\Delta x)^2} + \frac{U_{i,j+1}^{k+1} + U_{i,j-1}^{k+1} + U_{i,j+1}^{k} - 2U_{i,j}^{k} + U_{i,j-1}^{k}}{2(\Delta z)^2} \right) \right] \Bigg/$$
$$\left[\frac{1}{\Delta t} + \frac{U_{i+1,j}^{k+1} - U_{i-1,j}^{k+1} + U_{i+1,j}^{k} - U_{i-1,j}^{k}}{4(\Delta x)} + \frac{1}{Re\,(\Delta x)^2} + + \frac{1}{Re\,(\Delta z)^2} + M + X \right] \tag{3.5.7}$$

The finite difference approximations of $\frac{\partial W}{\partial t}$, $\frac{\partial W}{\partial x}$, $\frac{\partial W}{\partial z}$, $\frac{\partial^2 W}{\partial x^2}$, and $\frac{\partial^2 W}{\partial z^2}$ obtained at k and k+1 are given by:

$$\frac{\partial W}{\partial t} = \frac{W_{i,j}^{k+1} - W_{i,j}^{k}}{\Delta t} \tag{3.5.8}$$

$$\frac{\partial W}{\partial x} = \frac{W_{i+1,j}^{k+1} - W_{i-1,j}^{k+1} + W_{i+1,j}^{k} - W_{i-1,j}^{k}}{4(\Delta x)} \tag{3.5.9}$$

$$\frac{\partial W}{\partial y} = \frac{W_{i,j+1}^{k+1} - W_{i,j-1}^{k+1} + W_{i,j+1}^{k} - W_{i,j-1}^{k}}{4(\Delta z)} \tag{3.5.10}$$

$$\frac{\partial^2 W}{\partial x^2} = \frac{W_{i+1,j}^{k+1} - 2W_{i,j}^{k+1} + W_{i-1,j}^{k+1} + W_{i+1,j}^{k} - 2W_{i,j}^{k} + W_{i-1,j}^{k}}{2(\Delta x)^2} \tag{3.5.11}$$

$$\frac{\partial^2 W}{\partial z^2} = \frac{W_{i,j+1}^{k+1} - 2W_{i,j}^{k+1} + W_{i,j-1}^{k+1} + W_{i,j+1}^{k} - 2W_{i,j}^{k} + W_{i,j-1}^{k}}{2(\Delta z)^2} \tag{3.5.12}$$

Substituting these in equation of momentum (3.4.23) yields

$$\begin{aligned}
&\frac{W_{i,j}^{k+1}-W_{i,j}^{k}}{\Delta t}+U_{i,j}^{k+1}\left(\frac{W_{i+1,j}^{k+1}-W_{i-1,j}^{k+1}+W_{i+1,j}^{k}-W_{i-1,j}^{k}}{4(\Delta x)}\right)+\\
&w_0\left(\frac{W_{i,j+1}^{k+1}-W_{i,j-1}^{k+1}+W_{i,j+1}^{k}-W_{i,j-1}^{k}}{4(\Delta z)}\right)\\
&=\frac{1}{Re}\left(\frac{W_{i+1,j}^{k+1}-2W_{i,j}^{k+1}+W_{i-1,j}^{k+1}+W_{i+1,j}^{k}-2W_{i,j}^{k}+W_{i-1,j}^{k}}{2(\Delta x)^2}\right)\\
&+\frac{1}{Re}\left(\frac{W_{i,j+1}^{k+1}-2W_{i,j}^{k+1}+W_{i,j-1}^{k+1}+W_{i,j+1}^{k}-2W_{i,j}^{k}+W_{i,j-1}^{k}}{2(\Delta z)^2}\right)-XW_{i,j}^{k+1}
\end{aligned} \tag{3.5.13}$$

Making $W_{i,j}^{k+1}$ yields:

$$\begin{aligned}
W_{i,j}^{k+1}=&\left[\frac{W_{i,j}^{k}}{\Delta t}-w_0\left(\frac{W_{i,j+1}^{k+1}-W_{i,j-1}^{k+1}+W_{i,j+1}^{k}-W_{i,j-1}^{k}}{4(\Delta z)}\right)-U_{i,j}^{k+1}\left(\frac{W_{i+1,j}^{k+1}-W_{i-1,j}^{k+1}+W_{i+1,j}^{k}-W_{i-1,j}^{k}}{4(\Delta x)}\right)+\right.\\
&\left.\frac{1}{Re}\left(\frac{W_{i+1,j}^{k+1}+W_{i-1,j}^{k+1}+W_{i+1,j}^{k}-2W_{i,j}^{k}+W_{i-1,j}^{k}}{2(\Delta x)^2}+\frac{W_{i,j+1}^{k+1}+W_{i,j-1}^{k+1}+W_{i,j+1}^{k}-2W_{i,j}^{k}+W_{i,j-1}^{k}}{2(\Delta z)^2}\right)\right]\Bigg/\\
&\left[\frac{1}{\Delta t}+\frac{1}{Re\,(\Delta x)^2}+\frac{1}{Re\,(\Delta z)^2}+X\right]
\end{aligned} \tag{3.5.14}$$

The finite difference approximations of $\frac{\partial T}{\partial t}$, $\frac{\partial T}{\partial x}$, $\frac{\partial T}{\partial z}$, $\frac{\partial^2 T}{\partial x^2}$, and $\frac{\partial^2 T}{\partial z^2}$ obtained at k and k+1 are given by:

$$\frac{\partial T}{\partial t}=\frac{T_{i,j}^{k+1}-T_{i,j}^{k}}{\Delta t} \tag{3.5.15}$$

$$\frac{\partial T}{\partial x}=\frac{T_{i+1,j}^{k+1}-T_{i-1,j}^{k+1}+T_{i+1,j}^{k}-T_{i-1,j}^{k}}{4(\Delta x)} \tag{3.5.16}$$

$$\frac{\partial T}{\partial z}=\frac{T_{i,j+1}^{k+1}-T_{i,j-1}^{k+1}+T_{i,j+1}^{k}-T_{i,j-1}^{k}}{4(\Delta z)} \tag{3.5.17}$$

$$\frac{\partial^2 T}{\partial x^2}=\frac{T_{i+1,j}^{k+1}-2T_{i,j}^{k+1}+T_{i-1,j}^{k+1}+T_{i+1,j}^{k}-2T_{i,j}^{k}+T_{i-1,j}^{k}}{2(\Delta x)^2} \tag{3.5.18}$$

$$\frac{\partial^2 T}{\partial z^2} = \frac{T_{i,j+1}^{k+1} - 2T_{i,j}^{k+1} + T_{i,j-1}^{k+1} + T_{i,j+1}^{k} - 2T_{i,j}^{k} + T_{i,j-1}^{k}}{2(\Delta z)^2} \tag{3.5.19}$$

Substituting these in equation of energy (3.4.24) yields

$$\begin{aligned}
&\frac{T_{i,j}^{k+1} - T_{i,j}^{k}}{\Delta t} + U_{i,j}^{k+1}\left(\frac{T_{i+1,j}^{k+1} - T_{i-1,j}^{k+1} + T_{i+1,j}^{k} - T_{i-1,j}^{k}}{4(\Delta x)}\right) + \\
&W_{i,j}^{k+1}\left(\frac{T_{i,j+1}^{k+1} - T_{i,j-1}^{k+1} + T_{i,j+1}^{k} - T_{i,j-1}^{k}}{4(\Delta z)}\right) \\
&= \frac{1}{RePr}\left(\frac{T_{i+1,j}^{k+1} - 2T_{i,j}^{k+1} + T_{i-1,j}^{k+1} + T_{i+1,j}^{k} - 2T_{i,j}^{k} + T_{i-1,j}^{k}}{2(\Delta x)^2}\right) \\
&+ \frac{1}{RePr}\left(\frac{T_{i,j+1}^{k+1} - 2T_{i,j}^{k+1} + T_{i,j-1}^{k+1} + T_{i,j+1}^{k} - 2T_{i,j}^{k} + T_{i,j-1}^{k}}{2(\Delta z)^2}\right) + \\
&ReR\left(U_{i,j+1}^{k+1}\right)^2 + \frac{Ec}{Re}\left(\frac{U_{i+1,j}^{k+1} - U_{i-1,j}^{k+1} + U_{i+1,j}^{k} - U_{i-1,j}^{k}}{4(\Delta x)}\right)^2 + \\
&\frac{Ec}{Re}\left(\frac{W_{i,j+1}^{k+1} - W_{i,j-1}^{k+1} + W_{i,j+1}^{k} - W_{i,j-1}^{k}}{4(\Delta z)}\right)^2
\end{aligned} \tag{3.5.20}$$

Making $T_{i,j}^{k+1}$ yields:

$$\begin{aligned}
T_{i,j}^{k+1} = &\left[\frac{T_{i,j}^{k}}{\Delta t} - U_{i,j}^{k+1}\left(\frac{T_{i+1,j}^{k+1} - T_{i-1,j}^{k+1} + T_{i+1,j}^{k} - T_{i-1,j}^{k}}{4(\Delta x)}\right) - W_{i,j}^{k+1}\left(\frac{T_{i,j+1}^{k+1} - T_{i,j-1}^{k+1} + T_{i,j+1}^{k} - T_{i,j-1}^{k}}{4(\Delta z)}\right) + \right. \\
&\frac{1}{RePr}\left(\frac{T_{i+1,j}^{k+1} + T_{i-1,j}^{k+1} + T_{i+1,j}^{k} - 2T_{i,j}^{k} + T_{i-1,j}^{k}}{2(\Delta x)^2}\right) + \frac{1}{RePr}\left(\frac{T_{i,j+1}^{k+1} + T_{i,j-1}^{k+1} + T_{i,j+1}^{k} - 2T_{i,j}^{k} + T_{i,j-1}^{k}}{2(\Delta z)^2}\right) + \\
&\left. ReR\left(U_{i,j+1}^{k+1}\right)^2 + \frac{Ec}{Re}\left(\frac{U_{i+1,j}^{k+1} - U_{i-1,j}^{k+1} + U_{i+1,j}^{k} - U_{i-1,j}^{k}}{4(\Delta x)}\right)^2 + \frac{Ec}{Re}\left(\frac{W_{i,j+1}^{k+1} - W_{i,j-1}^{k+1} + W_{i,j+1}^{k} - W_{i,j-1}^{k}}{4(\Delta z)}\right)^2\right] \Bigg/ \left[\frac{1}{\Delta t} + \right. \\
&\left.\frac{1}{RePr\,(\Delta x)^2} + \frac{1}{RePr\,(\Delta z)^2}\right]
\end{aligned} \tag{3.5.21}$$

3.5.2 Advantages of using finite difference method

1. It is stable and of rapid covergence

2. It is accurate

3. It is a very versatile modelling technique which is comparatively easy for users to understand and implement.

Equations (3.6.7), (3.6.14) and (3.6.21) were simulated in MATLAB to obtain the profiles. The MATLAB code version 7.9.0(R2019b) is at the end of the document.

CHAPTER FOUR

RESULTS AND DISCUSSIONS

4.1 Introduction

This chapter presents the results of temperature and velocity profiles for the model while varying various dimensionless parameters and then discussing them at each step. Momentum equation in x-direction (3.6.7), z-direction (3.6.14) and energy equation(3.6.21) are solved using the MATLAB version 7.9.0(R2019b). Varying various non-dimensional parameters produced graphs which were discussed into details.

4.2 Results and Discussions

4.2.1 A graph showing the effects of varying Reynolds number on primary velocity

From the Figure 4.1, it is noted that when Reynolds number is raised then the primary velocity profile rises. Since Reynolds number represents the ratio of inertial forces to viscosity forces, then an increase in Reynolds number is due to an increase in inertia forces and a decrease in viscous forces. The force that opposes the motion of the fluid is viscous force, therefore if Reynolds number(Re) is small, it means that the viscous forces are more dominant than the inertial forces and thus causes more drag in the fluid thereby a reduction in the flow velocity.

4.2.2 A graph showing the effects of varying Magnetic number on primary velocity

From Figure 4.2, it is noted that when a magnetic parameter increases, then there is a corresponding decrease in primary velocity of the flowing fluid. This is due to the presence of Lorentz force that

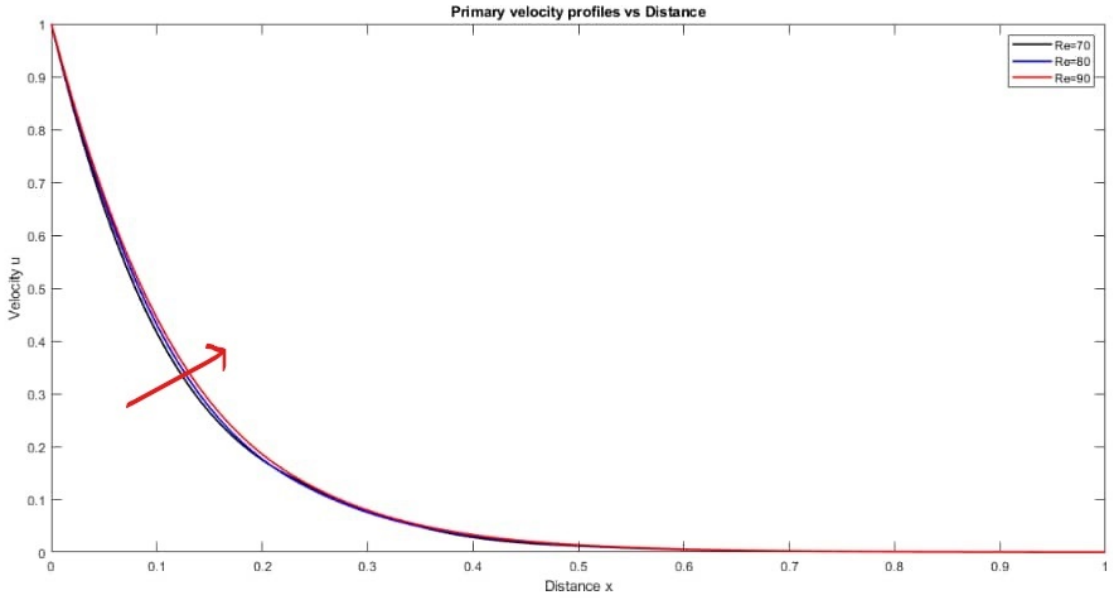

Figure 4.1: Velocity profiles for varied values of the Reynolds number, Re.

is caused by magnetic field acting normally to the fluid. The Lorentz force opposes the motion of the flow since it acts on opposite direction.

4.2.3 A graph showing the effects of varying permeability parameter on primary velocity

From Figure 4.3, it is observed that increase in primary velocity profile is due to a decrease in permeability parameter (X). Increased porosity of the medium increases the permeability parameter thereby reducing the fluid flow acceleration. Increased permeability reduces the acceleration of the fluid flowing since the pores that would have allowed the fluid to flow with less restriction closes and as a result the primary velocity decreases.

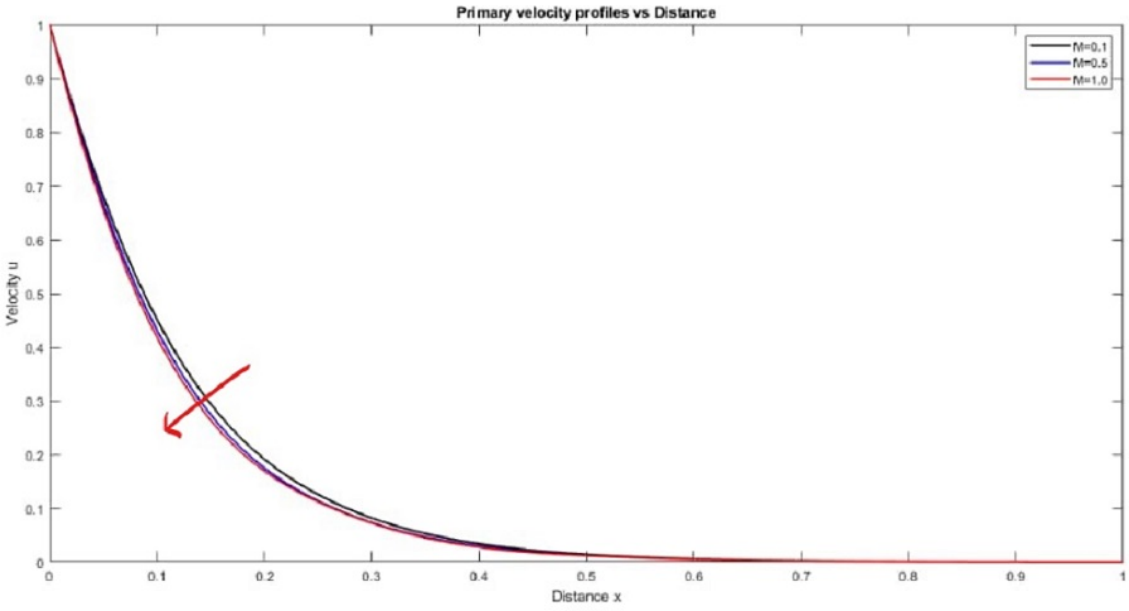

Figure 4.2: Velocity profiles for varied values of the Magnetic number, M.

4.2.4 A graph showing the effects of varying Reynolds number on secondary velocity, Re

From the Figure 4.4, it is noted that secondary velocity increases due to increase in Reynolds number. When the viscous forces reduces then there will be a reduction in the opposition of the motion of the fluid therefore the fluid velocity increases and when the inertial forces reduces then Reynolds number will decrease which means that there will be dominant viscous forces.

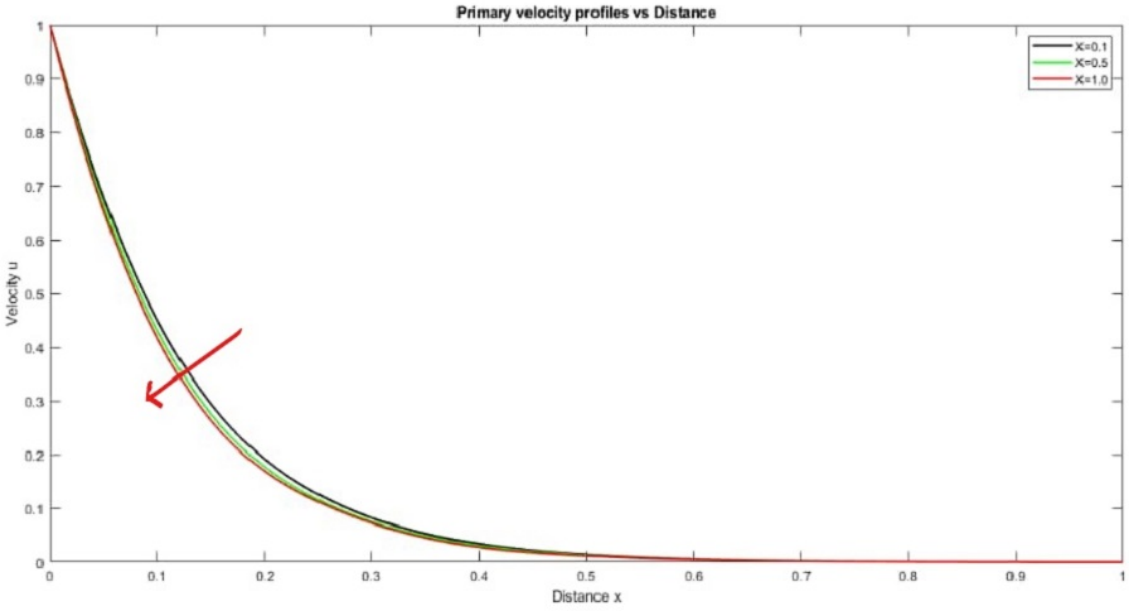

Figure 4.3: Velocity profiles for varied values of the X number.

4.2.5 A graph showing the effects of varying permeability parameter on secondary velocity

From Figure 4.5, it is noted that decrease in secondary velocity profile is due to increased permeability parameter (X). Increased porosity of the medium raises the permeability parameter which causes a reduction in acceleration of the flow. Hence reduction in secondary velocity profile.

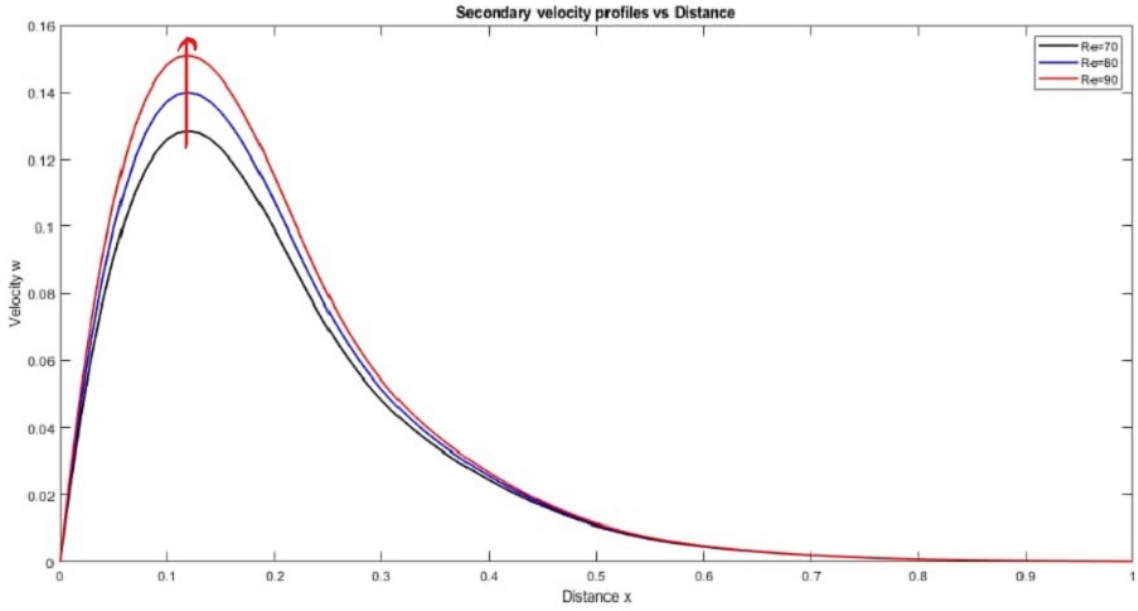

Figure 4.4: Velocity profiles for varied values of the Reynolds number, Re.

4.2.6 A graph showing the effects of varying Prandtl number on Temperature profile

From Figure 4.6, it is noted that a rise in the temperature profiles is due to increase in Prandtl number. Prandtl number is defined as the ratio of viscous diffusion rate to thermal diffusion. Increase in Prandtl number means low thermal diffusivity of the fluid which leads to increased internal temperature of the fluid.

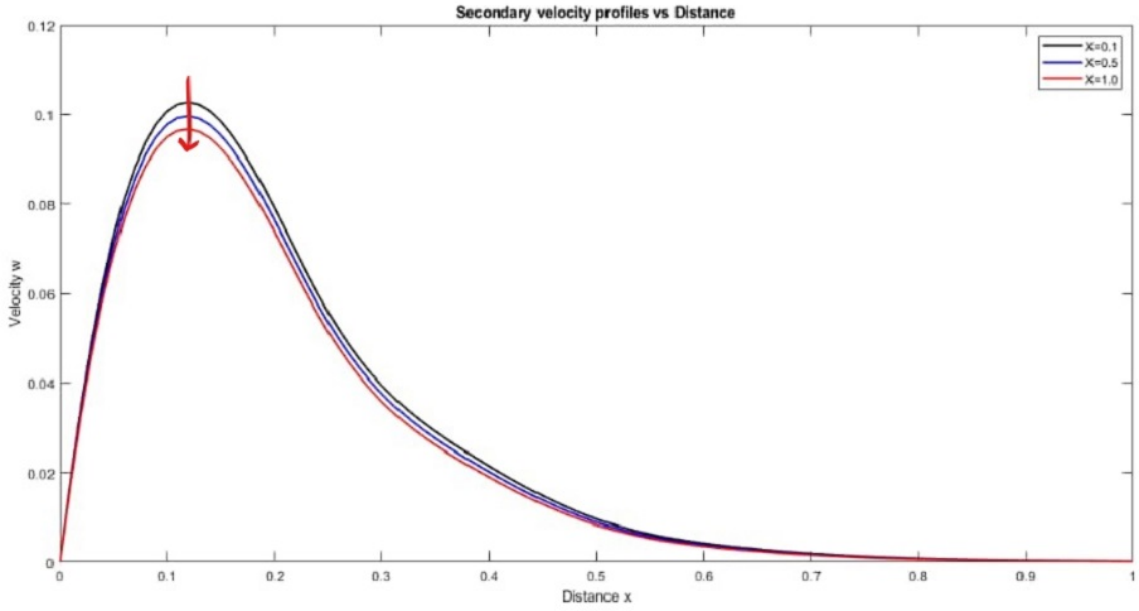

Figure 4.5: Velocity profiles for varied values of the x number.

4.2.7 A graph showing the effects of varying Reynolds number on Temperature profile

From the graph 4.7, it is noted that temperature profiles increases if there is an increase in Reynolds number. A decrease in viscous forces means that there is reduced inertial forces thereby leading to increased motion of particles of the fluid. Heat is generated due to collision of the particles which are moving at high velocity thereby increasing the fluids temperature.

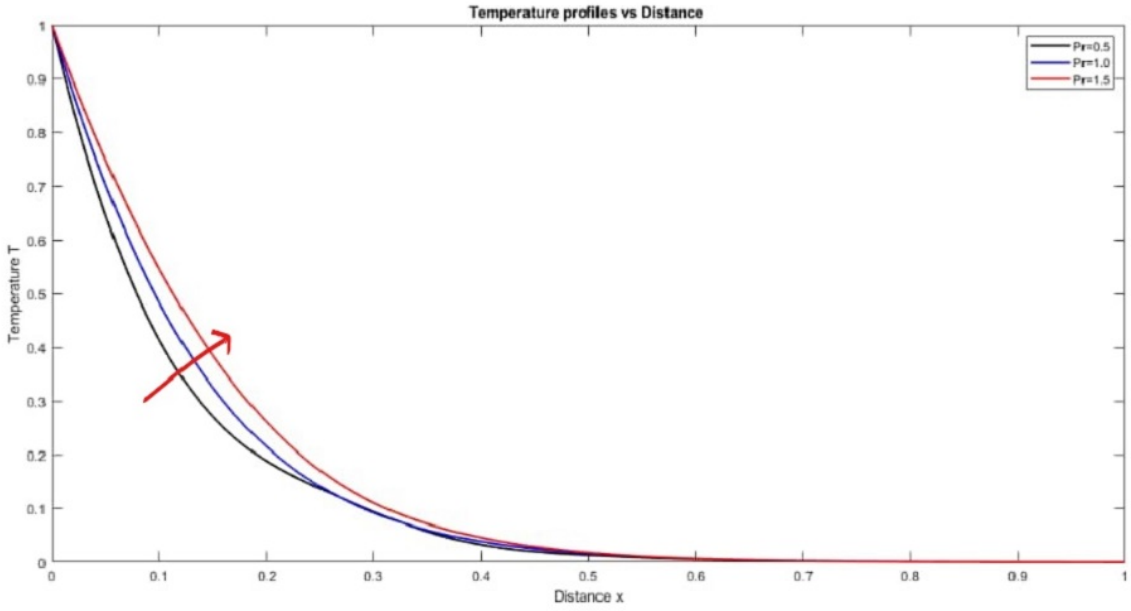

Figure 4.6: Temperature profiles for varied values of the Pr number.

4.2.8 A graph showing the effects of varying Eckert number on Temperature profile

From Figure 4.8, it is noted that the temperature profiles increases when the Eckert number (Ec) is increased. A rise in the Eckert number translates into increased kinetic energy of the fluid. This increases the motion of the fluids particles which collides and generates energy thereby making the fluids temperature to rise.

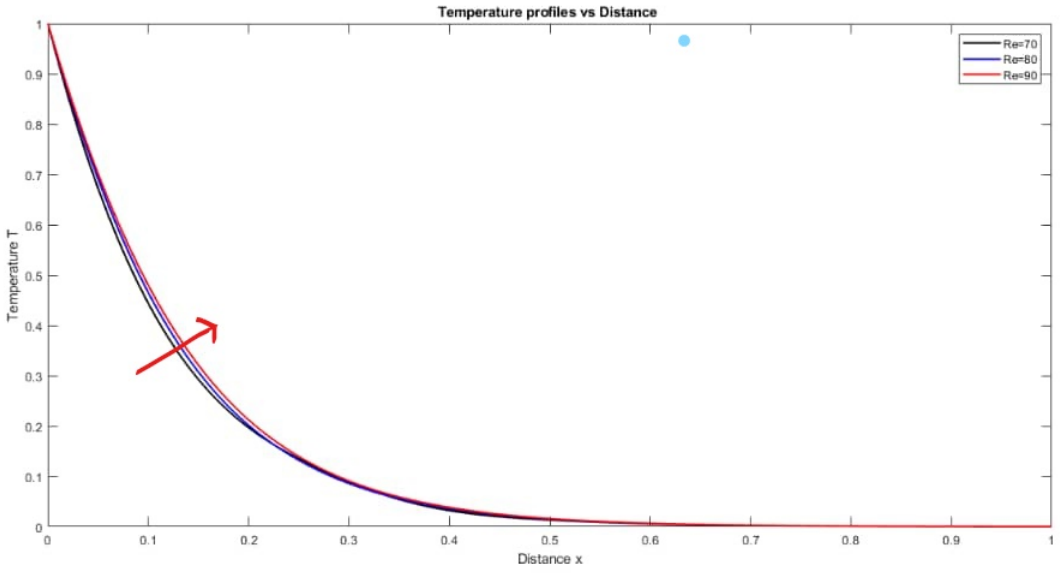

Figure 4.7: Temperature profiles for varied values of the Re number.

4.2.9 A graph showing the effects of varying Joule heating parameter (R) Temperature profile

From Figure 4.9, it is noted that increase in joule heating parameter (R) leads to an increased in temperature. As the current is induced and starts flowing in the fluid, heat is generated due to the electrical resistance to the flow of charges thereby increasing the temperature.

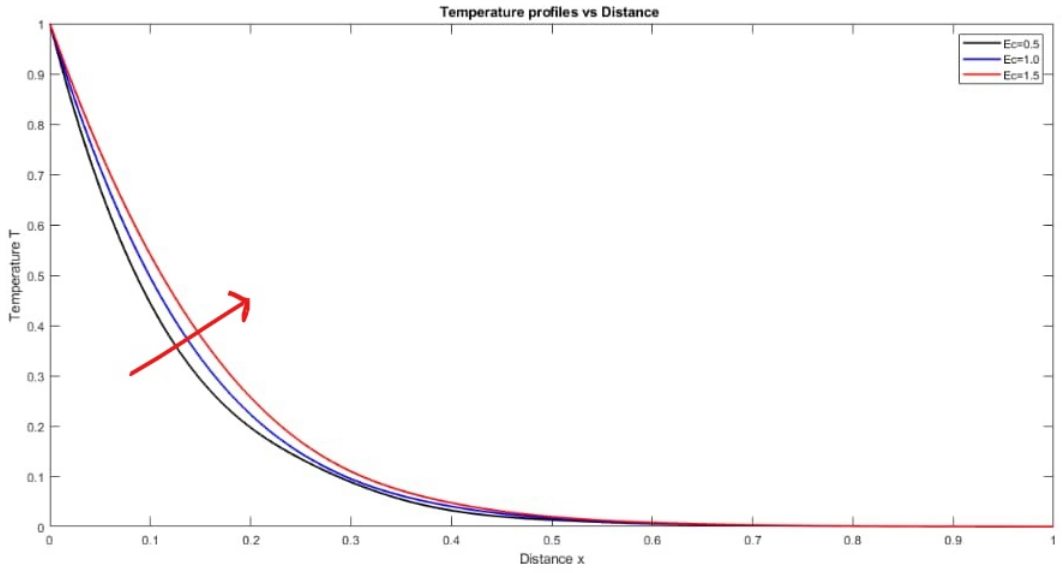

Figure 4.8: Temperature profiles for varied values of the Ec number.

4.3 Validation of Results

This result agrees with (Job and Gunakala, 2016), when there is absence of thermal radiation. There findings were;

1. When the Eckert number (Ec) was increased the temperature and velocity profiles also increased.
2. The temperature and velocity profiles increased when Prandtl number was increased.
3. A rise in magnetic parameter increased the temperature profiles.

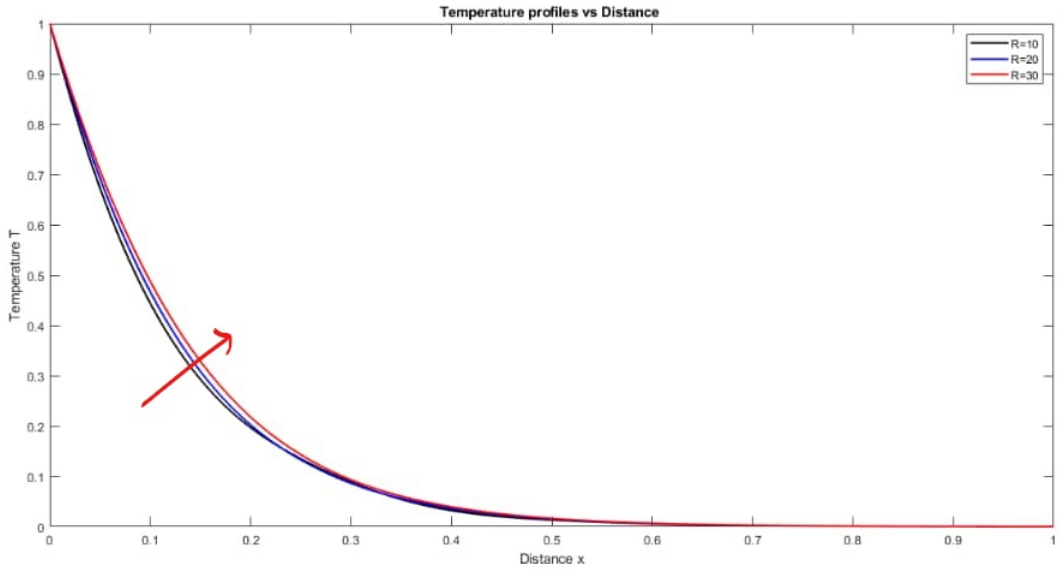

Figure 4.9: Temperature profiles for varied values of the R number.

CHAPTER FIVE

CONCLUSION AND RECOMMENDATIONS

5.1 Introduction

This chapter presents a summary of what has been done to attain the objectives and also recommendations for future research has been presented.

5.2 Conclusions

The results of this study leads to conclusion that;

1. Increase in Reynolds number has an accelerating influence on the primary and secondary velocity of the flow.

2. Increase in suction and injection parameters leads to decrease in primary flow.

3. Temperature of the flow was affected by Joule Heating parameter (R), Eckert number (Ec) and Prandtl number (Pr) where by their increase led to increase in temperature of the fluid.

4. Magnetic number and permeability parameter exerts a retarding influence on the fluid primary and secondary velocity when they are increased.

5.3 Recommendations

The study of hydromagnetic Couette flow between two vertical semi-infinite permeable plates with uniform suction and injection still needs further research. Therefore, my recommendations are;

1. Unsteady hydromagnetic turbulent flow through two vertical infinite plates.
2. Steady hydromagnetic three dimensional Couette flow between vertical finite permiable plates with variable magnetic field at an angle.
3. Unsteady MHD compressible flow past pearmeable vertical plates with chemical reaction.

REFERENCES

Ahmed, F. H. A. (2015). *Effect of Silver Nitrate Concentrations on pH of Water*. Doctoral dissertation, Sudan University Of Science & Technology Repository.

Anderson, J. D. (2007). Introduction: Downwash and induced drag. *Fundamentals of Aerodynamics*, Tata McGraw-Hill Education, 395–400.

Attia, H. A. (2018). Unsteady MHD Couette flow of a viscoelastic fluid with heat transfer. *Kragujevac J. Sci, 32*, 5–15.

Attia, H. A. and Ewis, K. M. (2010). Unsteady MHD Couette flow with heat transfer of a viscoelastic fluid under exponential decaying pressure gradient. *Int. J. Appl. Math. Mech, 13(4)*, 359–364.

Bodosa, G. and Borkakati, A. (2017). MHD flow with heat transfer between two horizontal plates in the presence of a uniform transverse magnetic field. *Theoretical and Applied Mechanics, 30(1)*, 1–9.

Boniface, K., Jackson, K., and Thomas, O. (2014). Investigation of hydro magnetic steady flow between two infinite parallel vertical porous plates. *American Journal of Applied Mathematics, 2(5)*, 170–178.

Chandran, P., Sacheti, N. C., and Singh, A. (2017). Effect of rotation on unsteady hydromagnetic Couette flow. *Astrophysics and Space Science, 202(1)*, 1–10.

Chauhan, D. S. and Agrawal, R. (2015). Effects of hall current on MHD flow in a rotating channel. *Chemical Engineering Communications, 197(6)*, 830–845.

De Andrade, V. and Pereira, J. (2015). Gravitational lorentz force and the description of the gravitational interaction. *Physical Review D, 56(8)*, 4689.

Freidoonimehr, N., Rashidi, M. M., and Mahmud, S. (2015). Unsteady MHD free convective flow past a stretching vertical porous surface. *International Journal of Thermal Sciences, 87*, 136–145.

Jha, B. K., Samaila, A. K., and Ajibade, A. O. (2015). Unsteady natural convection Couette flow of a reactive viscous fluid in a vertical channel. *Computational Mathematics and Modeling, 24(3)*, 432–442.

Job, V. M. and Gunakala, S. R. (2016). Unsteady mhd free convection Couette flow between two vertical permeable plates in the presence of thermal radiation using galerkin's finite element method. *International Journal of Mechanical Engineering, 2(5)*, 99–110.

Johana, S. K., Okelo, J., Gatheri, F. K., Ngesa, J. O. (2018). MHD flow past a porous infinite vertical plate. vertical porous plate with joule heating. *Scientific Research Journal, 4(5)*, 825–833

Joseph, K., Daniel, S., and Joseph, G. (2015). Unsteady MHD flow through two infinite parallel porous plates where there is an inclined magnetic field with heat transfer. *International Journal of Mathematics and Statistics Invention, 2(3)*, 103–110.

Muhuri, P. (2018). Flow formation in Couette motion in magnetohydrodynamics with suction. *J. Phys. Soci. J, 18(11)*, 1671–1675.

Kim, Y. J. (2018). MHD flow past a semi-infinite porous vertical moving plate with variable suction. *International journal of engineering science, 38(8)*, 833–845.

Kinyanjui, M., Chaturvedi, N., and Uppal, S. (2013). Stokes problem for an infinite vertical plate with hall current. *Energy conversion and Management, 39(n5-6)*, 541–548.

Makinde, O. and Mhone, P. (2019). Heat transfer to mhd oscillatory flow in a channel filled with porous medium. *Romanian Journal of physics, 50(n9-10)*, 931.

Onyango, E. R and Kinyanjui, M. N and Kimathi, M (2015). Effects of Direction of Transverse Magnetic Field on MHD Couette Flow. *International Journal of Education and Research, 4(2)*, 150

Onyango, E. R and Kinyanjui, M. N and Uppal, S. M (2017). Unsteady hydromagnetic Couette flow with the magnetic field being fixed on the side of the moving upper plate. *American Journal of Applied Mathematics, 3(5), 206*

Mukhopadhyay, S. (2016). The analysis of a boundary layer flow over a porous non-linearly stretching sheet with partial slip at the boundary. *Alexandria Engineering Journal, 52(4)*, 563–569.

Rajput, U. and Sahu, P. (2016). Natural convection in unsteady hydromagnetic Couette flow through a channel in the presence of thermal radiation. *Int. J. Appl. Math. Mech, 8(3)*, 35–56.

Raptis, A. and Kafousias, N. (2015). Magnetohydrodynamic free convective flow and mass transfer through a medium bounded by an infinite vertical permeable plate with constant heat flux. *Canadian Journal of Physics, 60(12)*, 1725–1729.

Seth, G., Ansari, M. S., and Nandkeolyar, R. (2017). Effects of rotation and magnetic field on unsteady Couette flow in a porous channel. *Journal of Applied Fluid Mechanics, 4(2)*, 95–103

Steenbrink, A. and Van der Giessen, E. (2016). On cavitation, post-cavitation and yield in amorphous polymer–rubber blends. *Journal of the Mechanics and Physics of Solids, 47(4)*, 843–876.

APPENDICES

Appendix I: Published Article

Owuor, O. C., Kinyanjui, M. N., & Kiogora, P. R. (2020). Hydromagnetic Couette Flow between Two Vertical Semi-Infinite Permeable Plates. *International Journal of Advances in Applied Mathematics and Mechanics*, 7, 1-13.

Appendix II: MATLAB Codes

MAIN FUNCTION

function[u,w,T,x]=Adriel(M,X,Ec,Pr,Re,Gr,R,wo) clc

str=1; n=2;

xmax=1;zmax=1;tmax=1;xsteps=32;zsteps=64; tsteps=1000;

x = linspace(0,1,xsteps-23); y = linspace(0,1,xsteps-22);

p = linspace(0,1,xsteps-1); u= zeros(xsteps,tsteps);

w= zeros(xsteps,tsteps); T= zeros(xsteps,tsteps);

dx=0.005; dz=0.005; dt=0.001; rem boundary conditions

initial

for i=1:xsteps for j=1:zsteps for k=1:tsteps u(i,j,1)=0; w(i,j,1)=0; T(i,j,1)=1; end end end for i=2:xsteps for j=1:zsteps for k=2:tsteps

u(i,1,k)=1; w(i,1,k)=0 ; T(i,1,k)=0; end end end

for i=2:xsteps for j=2:zsteps for k=2:tsteps

$u(i,zsteps,k) = i*str*(dx)^n$; w(i,zsteps,k)=0.0; T(i,zsteps,k)=1;

end end end

for i=1:xsteps for j=2:zsteps for k=2:tsteps

u(1,j,k)=1; w(1,j,k)=0; T(1,j,k)=1; end end end

Solving for velocities and temperature

for i=2:xsteps-1 for j=2:zsteps-1 for k=2:tsteps-1 $u(i,j,k+1) = (u(i,j,k)/dt - (wo/(4*dz))*$

$(u(i,j+1,k+1) - u(i,j-1,k+1) + u(i,j+1,k) - u(i,j-1,k)) + Gr*T(i,j,k+1) + (1/(2*Re*$

$dx^2))*(u(i+1,j,k+1) + u(i-1,j,k+1) + u(i+1,j,k) + u(i-1,j,k) - 2*u(i,j,k)) + (1/(2*$

$Re*dz^2))*(u(i,j+1,k+1)+$

$u(i,j-1,k+1) + u(i,j+1,k) + u(i,j-1,k) - 2*u(i,j,k)))/(1/dt + (1/(4*dx))*(u(i+1,j,k+$

$1)-u(i-1,j,k+1)+u(i+1,j,k)-u(i-1,j,k))+1/(Re*dx^2)+1/(Re*dz^2)+X+M);$

$w(i,j,k+1)=(u(i,j,k)/dt-(u(i,j,k+1)/(4*dx))*(w(i+1,j,k+1)-w(i-1,j,k+1)+w(i+1,j,k)-w(i-1,j,k))-wo*(1/(4*dz))*(w(i,j+1,k+1)-w(i,j-1,k+1)+w(i,j+1,k)-w(i,j-1,k))+(1/(2*Re*dx^2))*(w(i+1,j,k+1)+w(i-1,j,k+1)+w(i+1,j,k)+w(i-1,j,k)-2*w(i,j,k))+(1/(2*Re*dz^2))*(w(i,j+1,k+1)+w(i,j-1,k+1)+w(i,j+1,k)+w(i,j-1,k)-2*w(i,j,k)))/(1/dt+1/(Re*dx^2)+1/(Re*dz^2)+X);$ $T(i,j,k+1)=(T(i,j,k)/dt-u(i,j,k+1)*(1/(4*dx))*(T(i+1,j,k+1)-T(i-1,j,k+1)+T(i+1,j,k)-T(i-1,j,k))-w(i,j,k+1)*(1/(4*dz))*(T(i,j+1,k+1)-T(i,j-1,k+1)+T(i,j+1,k)-T(i,j-1,k))+(1/(2*Re*Pr*dx^2))*(T(i+1,j,k+1)+T(i-1,j,k+1)+T(i+1,j,k)+T(i-1,j,k)-2*T(i,j,k))+(1/(2*Re*Pr*dz^2))*(T(i,j+1,k+1)+T(i,j-1,k+1)+T(i,j+1,k)+T(i,j-1,k)-2*T(i,j,k))+Re*R*(u(i,j,k+1))^2+((Ec)/(16*Re*dz^2))*(w(i,j+1,k+1)+w(i,j+1,k)-w(i,j-1,k+1)-w(i,j-1,k))^2+((Ec)/(Re))*((u(i+1,j,k+1)+u(i+1,j,k)-u(i-1,j,k+1)-u(i-1,j,k))/(4*dx))^2)/(1/dt+1/(Re*Pr*dx^2)+1/(Re*Pr*dz^2));$

end end end

PRIMARY PROFILES

figure(1) clc; clear; $[u,w,T,x]=Adriel(M,X,Ec,Pr,Re,Gr,R,wo)$ Changing Re $[u,w,T,x]=Adriel(10,20,0.5,0.71,70,0.5,0.5,0.05);$ x1= 0:0.01:1; y1=spline(x,u(1:9,10,10),x1); plot(x1 ,y1,' k' ,'Linewidth',1.5,'LineSmoothing','on'); title('Primary velocity profiles vs Distance'); xlabel('Distance x'); ylabel('Velocity u');

SECONDARY PROFILES

figure(2) hold on clc; clear; $[u,w,T,x]=Adriel(M,X,Ec,Pr,Re,Gr,R,wo)$ Changing Re $[u,w,T,x]=Adriel(10,20,0.5,0.71,70,0.5,0.5,0.05);$ x1= 0:0.01:1;

y1=spline(x,w(1:9,10,10),x1); plot(x1 ,y1,' k' ,'Linewidth',1.5,'LineSmoothing','on'); hold on $[u,w,T,x] = Adriel(10,20,0.5,0.71,80,0.5,0.5,0.05)$; x2= 0:0.01:1; y2=spline(x,w(1:9,10,10),x2); plot(x2 ,y2,' g' ,'Linewidth',1.5,'LineSmoothing','on'); hold on $[u,w,T,x] = Adriel(10,20,0.5,0.71,90,0.5,0.5,0.05)$; x3= 0:0.01:1; y3=spline(x,w(1:9,10,10),x3); plot(x3 ,y3,' b' ,'Linewidth',1.5,'LineSmoothing','on'); hold on $[u,w,T,x] = Adriel(10,20,0.5,0.71,100,0.5,0.5,0.05)$; x5= 0:0.01:1; y5=spline(x,w(1:9,10,10),x5); plot(x5 ,y5,' r' ,'Linewidth',1.5,'LineSmoothing','on'); title('Secondary velocity profiles vs Distance'); xlabel('Distance x'); ylabel('Velocity w'); legend('Re=70','Re=80','Re=90','Re=100') hold off

TEMPERATURE PROFILES

figure(3) $[u,w,T,x] = Adriel(10,20,0.5,0.71,60,0.5,0.5,0.05)$; x1= 0:0.01:1; y1=spline(x,T(1:9,10,10),x1); plot(x1 ,y1,' r' ,'Linewidth',1.5,'LineSmoothing','on'); title('Temperature profiles vs Distance '); xlabel('Distance x'); ylabel('Temperature T');